



Positive modulation of the TMEM16B mediated currents by TRPV4 antagonist

Adan Hernandez^{*}, Alfredo Alaniz-Palacios, Juan A. Contreras-Vite, Ataúlfo Martínez-Torres^{**}

Departamento de Neurobiología Celular y Molecular, Laboratorio de Neurobiología Molecular y Celular, Instituto de Neurobiología, Universidad Nacional Autónoma de México, Juriquilla, 76230 Santiago de Querétaro, Querétaro, Mexico

ARTICLE INFO

Keywords:

Calcium-activated chloride channels
TMEM16B channels
TRPV4 antagonist

ABSTRACT

Calcium-activated chloride channels (CaCCs) play important roles in many physiological processes and their malfunction is implicated in diverse pathologies such as cancer, asthma, and hypertension. TMEM16A and TMEM16B proteins are the structural components of the CaCCs. Recent studies in cell cultures and animal models have demonstrated that pharmacological inhibition of CaCCs could be helpful in the treatment of some diseases, however, there are few specific modulators of these channels. CaCCs and Transient Receptor Potential Vanilloid-4 (TRPV4) channels are co-expressed in some tissues where they functionally interact. TRPV4 is activated by different stimuli and forms a calcium permeable channel that is activated by GSK1016790A and antagonized by GSK2193874. Here we report that GSK2193874 enhances the chloride currents mediated by TMEM16B expressed in HEK cells at nanomolar concentrations and that GSK1016790A enhances native CaCCs of *Xenopus* oocytes. Thus, these compounds may be used as a tool for the study of CaCCs, TRPV4 and their interactions.

1. Introduction

Calcium-activated Chloride Currents were first described in *Xenopus laevis* oocytes [1,2], however, today is known that channels responsible for this current are broadly expressed in many tissues and cell types [3, 4]. Physiological roles of the CaCCs have been described in epithelial secretion [5], membrane excitability in cardiac muscle [6] and neurons [7], olfactory transduction [8], regulation of vascular tone [9], and photoreception [10].

TMEM16A and TMEM16B proteins are the structural components of CaCCs [11–13]. The structure of the mouse TMEM16A obtained by cryo-electron microscopy revealed that CaCCs are homodimers of subunits each containing its own pore [14,15]. CaCCs gating is a complex process involving the coupling of changes of intracellular Ca²⁺ concentrations, voltage membrane and extracellular chloride [16–18]. Protons [19] and lipids also regulate CaCCs activity [20,21].

These channels are present in several tissues where they play important functions and are involved in diverse pathologies [22–26]. This variety of functions has attracted attention to design selective drugs as therapeutic targets, for example, the pharmacological inhibition of CaCCs has been found to contribute to the treatment of diseases such as

asthma [4], hypertension [24,27] and cancer [28–30]. Diverse CaCCs blockers have been described, including fenamates (niflumic acid, flufenamic acid and mefenamic acid), tannic acid [31], MONNA [32], T16A_{inh}-A01 [33], CaCC_{inh}-A01 [34] and anthracene-9-carboxylic acid (A9C) [35], however, different reports have shown that these compounds have an effect on other channels such as CLC-K [36] and TRPA1 [37]; even flufenamic acid, a non-steroidal anti-inflammatory drug, has diverse molecular targets [38]. Niflumic acid is also commonly used to pharmacologically identify CaCCs, but it also blocks volume-regulated anion channels, K⁺ channels, and calcium currents [39–41]. Recently, Ani9 was reported like the most potent and selective small-molecule inhibitor of human ANO1 (TMEM16A), but does not affect ANO2 (TMEM16B) activity at the same concentration [42]. In summary, finding selectivity for TMEM16A and TMEM16B drugs still is a challenge.

Several reports have shown a pharmacological interaction of the CaCCs blockers with the transient receptor potential vanilloid subtypes channels (TRPV) [43], in consequence the physiological roles of TMEM16A are associated with TRPV1 and TRPV4 function [26,44]. This interaction is physiologically relevant and will be important to find selective drugs targeting TMEM16A, TMEM16B or TRPV channels for

^{*} Corresponding author.

^{**} Corresponding author.

E-mail addresses: adanherdez@inb.unam.mx (A. Hernandez), ataulfo@unam.mx (A. Martínez-Torres).

therapeutic treatments. An example of the complexity of this interaction is offered by the effects of the small molecule Eact, which was originally reported as a potent activator of TMEM16A, but later found to act as an activator of TRPV1 and TRPV4 channels [43,45]. These observations suggest pharmacological experiments on CaCCs and TRPV channels must be interpreted with caution and encourage opposite studies to assess the TRPV selective drugs effect onto TMEM16 ion channels.

TRPV4 channels are potently antagonized by GSK3527497, an orally-active, lipid-soluble highly selective compound with not known pharmacological off-targets [46] while GSK1016790A is a selective and potent agonist of the channel [47]. Here, we provide evidence that shows that GSK1016790A enhances the endogenous CaCCs of *X. laevis* oocytes while GSK2193874 at nanomolar concentrations enhances the currents mediated by TMEM16B channels expressed in HEK293 cells. These findings suggest a careful reinterpretation of the pharmacological effects observed with this TRPV4 antagonist *in vivo* and opens the possibility to use these molecules as template to design new selective drugs targeting TMEM16B.

2. Materials and methods

2.1. Oocyte recordings

All frogs were handled in accordance with the guidelines of the National Institute of Health Guide for Care and Use of Laboratory Animals and with the approval of the Institutional Animal Care and Use Committee of the Institute of Neurobiology, National Autonomous University of Mexico (UNAM). Ovarian lobes were removed from anesthetized *X. laevis* frogs and placed into Barth's saline solution (in mM): 88 NaCl, 1 KCl, 0.33 Ca₂(NO)₃, 0.41 CaCl₂, 0.82 MgSO₄, 2.4 NaHCO₃, 5 HEPES and 0.1 mg/mL gentamycin sulfate (pH 7.4). The follicular cell layer was removed manually and by treatment with collagenase type I (0.3 µg/µl) in Ca²⁺-free Ringer's solution at room temperature for 30 min; then, oocytes were washed 3–4 times and maintained at 16°C in Barth's solution.

All recordings were performed at room temperature using the two-microelectrode voltage-clamp technique [1]. Oocytes were placed into a recording chamber (0.5 mL volume) and perfused with Ringer's solution containing (in mM): 115 NaCl, 2 KCl, 1.8 CaCl₂, and 5 HEPES (pH 7.4) or modified Ringer's containing 106.8 NaCl, 2 KCl, 10 CaCl₂, and 5 HEPES (pH 7.4). Borosilicate glass micropipettes were made with a PUL-100 vertical pipette puller (World Precision Instruments, Sarasota, FL, USA) and filled with KCl 3 M (2–3 MΩ). Voltage-clamp recordings were performed with an AXOCAMP-2B amplifier and digitized with a Digidata 1440A controlled by pClamp 10.5 software for acquisition (Axon, Molecular Devices, LLC, Sunnyvale, CA, USA). Holding potential used was –60 mV and activation protocol was performed applying a stepwise square voltage depolarizing pulses from 10 mV to 50 mV preceded by a hyperpolarizing square pre-pulse at –100 mV.

2.2. Cell culture and transfection

Human embryonic kidney (HEK) 293 cells were grown in Dulbecco's modified Eagle medium (DMEM; GIBCO, Carlsbad, CA, USA) supplemented with 10% of FBS and 0.1% penicillin-streptomycin maintained at 37°C in 95%O₂ 5%/CO₂ atmosphere in a regular NU-4750 incubator (Nuair, Plymouth, MN, USA). The mouse TMEM16B cDNA (retinal isoform containing exon 13) was cloned into pEGFP-N1 vector. HEK293 cells seeded at low density on coverslips were transfected using lipofectamine 2000 Invitrogen reagent (Termofisher Scientific, Waltham, MA, USA) according to the protocol recommended by the manufacturer. Transfected cells were identified by the fluorescence and used for patch-clamp recordings after 12 h of transfection. Coverslips were placed into a recording chamber mounted on a stage of an inverted microscope (Olympus CKX41, Melville, NY, USA) equipped with a fluorescence and a mercury burner UV lamp (Olympus U-RFLT50).

2.3. Recording solutions

Pipette solution was prepared and calculated for free 2.5 µM Ca²⁺ concentration (based on equilibrium constants for EGTA chelation of Ca²⁺ and Mg²⁺; Winmaxc32 software, C. Patton, Stanford University, USA), according to the TMEM16B EC₅₀ reported [48]. Intracellular solution contained (in mM): 20.2 TEA-Cl, 9.9 CaCl₂, 50 HEPES, 85 sucrose and 25 HEDTA; adjusted to pH = 7.3 with TEA-OH. Extracellular solution contained (in mM): 139 TEA-Cl, 0.5 CaCl₂, 20 HEPES, 110 sucrose; adjusted to pH = 7.4 with TEA-OH. Niflumic acid, GSK1016790A and GSK2193874 compounds (from Sigma-Aldrich, St. Louis, MO) were prepared in DMSO, kept as stock solution 1000 times concentrated for each different concentration used, and stored at –20°C. Bath solution was used for dilution to obtain the Niflumic acid, GSK1016790A or GSK2193874 required concentrations.

2.4. Electrophysiological recordings

All recordings were performed at room temperature using the conventional whole-cell voltage-clamp technique. Micropipettes were made with borosilicate glass pulled in a P-97 puller (Sutter Instruments, Novato, CA, USA); the recording pipette used were 3–5 MΩ resistance filled with intracellular solution. All results were obtained at room temperature using the patch clamp whole-cell configuration, voltage-clamp recordings were obtained with an AXOPATCH 200B amplifier and digitized at 10 kHz with a Digidata 1322A controlled by the pClamp 10.5 software for acquisition (Axon, Molecular Devices, LLC, Sunnyvale, CA, USA). Membrane potential was held at 0 mV and stepwise square voltage pulses from –60 mV to +120 mV were applied to activate TMEM16B chloride currents.

2.5. Data analysis

Current activation (open) and deactivation (close) time constant was obtained by a standard mono exponential fitted taken the fast and initial part of the activation and deactivation current traces. Time courses of the current traces at different voltages were fitted by the following equation:

$$Y = A_1 \times e^{-t/\tau}$$

Here A₁ is the current amplitude and τ represents the time constant.

Voltage dependence of the channel opening was evaluated measuring the tail currents amplitude immediately after the activation pulse at different voltages and normalized respect to the maximal amplitude. Current-voltage curve was fitted by the following Boltzmann function to estimate the relative open probability:

$$I = (1 - I / I_{max}) / \left(1 + e^{((V - V_{1/2})/k)} \right)$$

Where V_{1/2} represents the voltage required for half-maximal activation; k represents the slope factor.

The concentration-response curve was built normalizing the current density obtained in presence of different GSKb concentrations of the control in absence of any drug. EC₅₀ was generated by fitting the data with a four-parameter sigmoidal curve equation using the Graphpad Prism software:

$$Y = Bottom + (Top - Bottom) / \left(1 + 10^{((\log EC_{50} - x) * Hillslope)} \right)$$

Where EC₅₀ is the concentration of agonist that gives a response halfway between Bottom and Top; Top and Bottom are plateaus in the units of the Y axis; and x = log(concentration).

All data were analyzed using Clampfit 10.7 (Axon, Molecular Devices, LLC, Sunnyvale, CA, USA), OriginLab (OriginLab Corporation, MA, USA) and GraphPad Prism 6.0 (GraphPad Software Inc., San Diego CA). An unpaired Student's *t*-test, Mann-Whitney *U* test or one-way

ANOVA with multiple comparisons correction, Tukey's post-hoc, were used to determine statistical significance. Experimental data points are presented as mean \pm S.E.M.

3. Results

3.1. CaCCs in *Xenopus* oocytes and TRPV4 agonist

The transient outward (*Tout*) chloride current described in *Xenopus* oocytes [1] is evident upon depolarization of the plasma membrane (from -120 mV to about $+20$ mV) which allows the influx of Ca^{2+} which in turn activates endogenously expressed CaCCs. The *Tout* current is greatly enhanced by increasing the external concentration of Ca^{2+} and in Fig. 1A we show sample traces of the *Tout* current in normal Ringer's and in Ringer's supplemented with 10 mM Ca^{2+} . In this condition, the

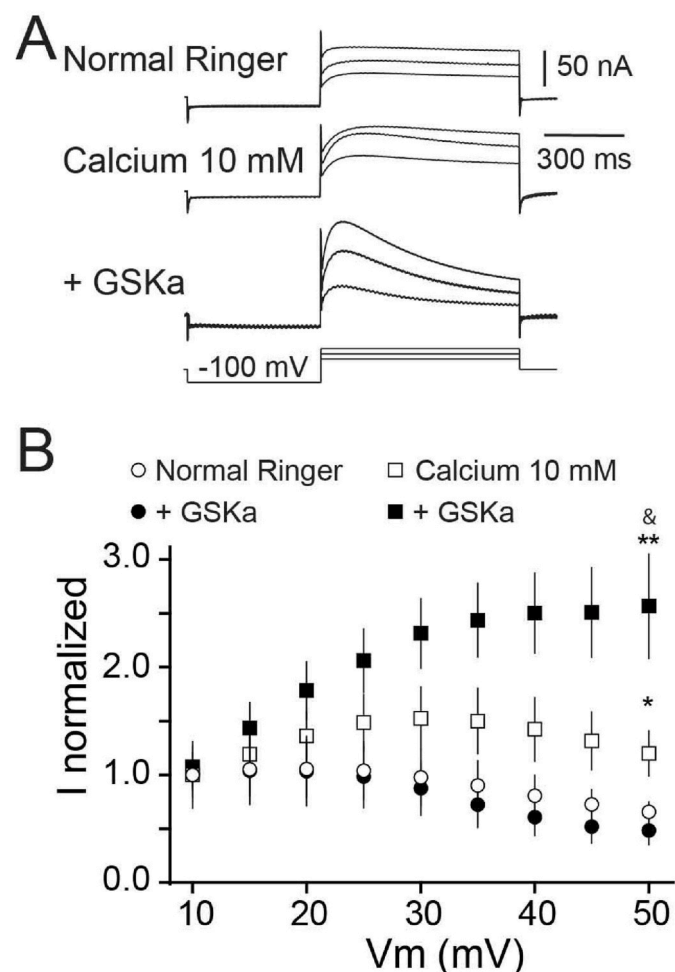


Fig. 1. Transient outward chloride current and TRPV4 modulation in *Xenopus* oocytes. (A) Representative current activation traces from *Xenopus* oocytes at different voltages (10, 30 and 50 mV) shows the absence of the transient outward current (*Tout*) in normal Ringer's solution (upper panel), the presence in Ringer's containing 10 mM calcium and enhancement in presence of calcium 10 mM plus GSK1016790A (+GSKa) (lower panel). (B) Summary of the current-voltage relation constructed from the maximal peak of the current amplitude measured from the initial activation and normalized respect to the peak amplitude at 10 mV. The effect of GSKa was statistically significant only in 10 mM calcium at positive voltages after 30 mV without effect in normal Ringer. * $p < 0.05$, ** $p < 0.01$, vs. Normal Ringer's; & $p < 0.05$ vs Calcium 10 mM; Unpaired student t -test; $n = 7$ Normal ringer, $n = 12$ calcium 10 mM, $n = 15$ +GSKa. empty circles (Normal Ringer), filled circles (Normal Ringer + GSKa), empty squares (calcium 10 mM), filled squares (calcium 10 mM + GSKa). Symbols show mean \pm S.E.M.

Tout current increased slowly in amplitude after the onset of the depolarizing pulse and reached a peak in a few milliseconds. Thus, in the following experiments the amplitude of the *Tout* current was maintained constant by increasing the extracellular Ca^{2+} concentration.

We first explored the action of the TRPV4 agonist GSK1016790A (GSKa) at 1 μM on the *Tout* current. GSKa did not elicit any evident effect on the oocytes in normal Ringer solution (Fig. 1B, filled circles), consistent with previous findings that did not detect expression of TRPV4 in oocytes [49]. Remarkably, the *Tout* current showed in extracellular 10 mM calcium is enhanced in presence of GSKa (Fig. 1A, +GSKa). Current amplitude was measured at the maximal transient peak after the slow activation induced by the square depolarizing pulses. Summary of the current-voltage relationship was constructed normalizing the peak amplitude to the amplitude measured at 10 mV for each condition, results show the maximal peak at 30 mV and decay at more positive voltages in 10 mM calcium (Fig. 1B). In the presence of GSKa the *Tout* was consistently enhanced and maintained up to $+50$ mV becoming statistically significant (2.6 ± 0.48 in GSKa vs. 1.2 ± 0.18 in control; * $p = 0.046$; unpaired student t -test; $n = 13, 7$, respectively) (Fig. 1B). In summary, this result indicates a positive modulation of the CaCCs by 1 μM of GSK1016790A in *Xenopus* oocytes. As mentioned above TMEM16A and TMEM16B are the molecular components that give rise to the CaCCs in *Xenopus* oocytes [50]. To explore whether GSKa targets a TMEM16 ion channels, we evaluated its effect on the cloned mouse TMEM16B mediated currents expressed in HEK293 cells.

3.2. Cloned mouse TMEM16B channels in HEK293 cells

First, we assessed the electrophysiological and pharmacological characteristic of TMEM16B. One of the most common blockers for native CaCCs are niflumic acid (N-A) and flufenamic acid, which block CaCCs in *Xenopus* oocytes at concentrations in the 10 μM range [51], however in HEK293 cells TMEM16B is not fully blocked even with 300 μM of N-A [48]. Expression of TMEM16B channels was evaluated in HEK293 cells, where the outward chloride currents were activated by depolarizing voltages that showed the typical activation and deactivation kinetics of TMEM16 channels (Fig. 2A). In this condition, the activation and deactivation time courses were clearly reduced without affecting the steady state current density in presence of N-A compared to control as is observed in the representative traces (Fig. 2A). Control recordings were obtained in presence of DMSO into the bath solution and our recordings were unchanged. Current density showing voltage dependency measured at the steady state current in different pharmacological conditions showed non-significant changes at the maximal voltage (control, 1011 ± 173.6 pA/pF, $n = 13$; N-A 10 μM , 1085 ± 271.7 pA/pF, $n = 7$; N-A 30 μM , 948.2 ± 132 pA/pF, $n = 7$) (Fig. 2B). Activation and deactivation time courses were measured by a single standard exponential fitted from the initial activation and deactivation current at positive voltages (40 – 120 mV). Control activation and deactivation time courses changed at different voltages; however, were not statistically significant. N-A pharmacological effect on TMEM16B currents increased the activation time course in a concentration dependent relation at all voltages explored (at 120 mV: control, 8.93 ± 0.63 ms, $n = 13$; N-A 10 μM , 27.23 ± 12.05 ms, $n = 7$, * $p = 0.0344$ vs control; N-A 30 μM , 111.2 ± 19.47 ms, $n = 7$, *** $p < 0.0001$ vs control, && $p = 0.0042$ vs NA 10 μM ; unpaired student t -test). Similarly, deactivation time course increased by N-A at all voltages in a concentration dependent relation (at 120 mV: control, 2.99 ± 0.72 ms, $n = 13$; N-A 10 μM , 9.03 ± 3.63 ms, $n = 7$, * $p = 0.0339$ vs control; N-A 30 μM , 38.2 ± 13.3 ms, $n = 7$, *** $p < 0.0004$ vs control, & $p = 0.047$ vs N-A 10 μM ; unpaired student t -test) (Fig. 2C). Normalized current voltage relation was built from tail currents normalized to the maximal amplitude in control and N-A at different concentrations. Boltzmann function was fitted to evaluate the voltage activation dependency and a shift to positive voltages was observed on the half-voltage activation in presence of N-A becoming significant at 30 μM concentration (control, 11.2 ± 3 mV, $n = 13$; N-A

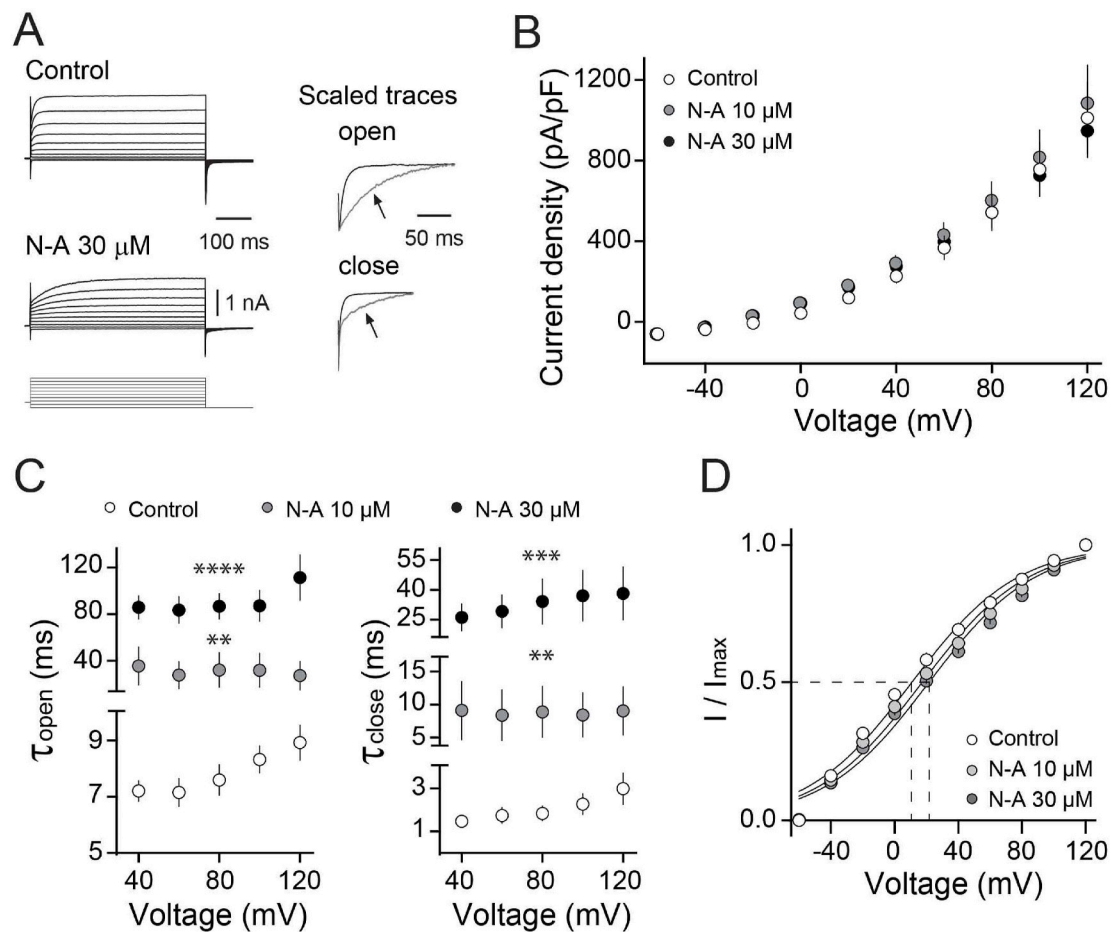


Fig. 2. Niflumic acid on TMEM16B currents in HEK293 cells. (A) Representative current traces induced by square voltage steps from -60 mV to $+120$ mV. Typical exponential activation and deactivation is observed in control conditions and niflumic acid (N-A). Activation and deactivation time course is shown on scaled traces for control (black) and $30 \mu\text{M}$ N-A (gray, pointed by arrow) at the right side of the panel. (B) Summary of the current-voltage relation (current density) constructed by measuring the current amplitude at the steady state shows similar voltage activation in all conditions. (C) Summary of the time constant of activation and deactivation currents taken from 40 mV to 120 mV. Activation and deactivation time constants were statistically increased in presence of N-A compared to control in concentration dependent relation. **** $p < 0.0001$, *** $p < 0.001$; N-A $30 \mu\text{M}$ vs. control, ** $p < 0.01$, N-A $10 \mu\text{M}$ vs. control; one-way ANOVA with multiple comparisons correction, Tukey's post-hoc. (D) Summary of the normalized current voltage relation from tail currents shows a shift to positive voltages (dashed lines) in presence of N-A fitted by the Boltzmann function (black lines). Symbols show mean \pm S.E.M.

$10 \mu\text{M}$, 17.9 ± 4.7 mV, $n = 7$, $p > 0.05$, vs control; N-A $30 \mu\text{M}$, 21.9 ± 2 mV, $n = 7$, * $p = 0.0365$, vs control; Mann-Whitney U test)(Fig. 2D). These results and the pharmacological effect on the activation and deactivation kinetics indicate that we recorded the typical calcium activated chloride current driven by TMEM16B transfected channels in HEK293 cells.

3.3. Effect of GSK1016790A on chloride currents mediated by TMEM16B channels

Once we obtained the electrophysiological profile of TMEM16B we next asked if the effect of GSKa observed in the oocyte *Tout* current was replicated in cloned TMEM16B. Outward chloride currents activated by depolarizing voltages showed the typical activation and deactivation kinetics in presence of different concentrations of GSKa (1 and $10 \mu\text{M}$, Fig. 3A). A current-voltage relation was obtained by measuring the steady-state current amplitude expressed as current density, where a slight increase was observed on the current density at 120 mV, however, it was not statistically significant (control, 1093 ± 152.4 pA/pF, $n = 10$; GSKa $1 \mu\text{M}$, 1348 ± 362.1 pA/pF, $n = 10$; GSKa $10 \mu\text{M}$, 1344 ± 313.2 pA/pF, $n = 8$) (Fig. 3B). Activation time course shows statistically significant increases at 120 mV (control, 10.39 ± 1.45 ms, $n = 10$; GSKa $1 \mu\text{M}$, 17.06 ± 2.47 ms, * $p = 0.032$, vs. control, $n = 10$; GSKa $10 \mu\text{M}$,

18.57 ± 3.98 ms, * $p = 0.025$, vs. control, $n = 8$; Unpaired student t -test), however it did not follow a concentration-dependent relation, similarly deactivation time course showed a significant increase at 120 mV (control, 7.55 ± 0.99 ms, $n = 10$; GSKa $1 \mu\text{M}$, 18.27 ± 4.15 ms, * $p = 0.0218$, vs. control, $n = 10$; GSKa $10 \mu\text{M}$, 13.15 ± 2.62 ms, * $p = 0.045$, vs. control, $n = 8$; Unpaired student t -test) (Fig. 3C). Boltzmann function was fitted to evaluate the voltage activation dependency on normalized current voltage relation from tail currents and non-significant change was observed on the half-voltage activation in presence of GSKa (control, 11.2 ± 3 mV, $n = 10$; GSKa $1 \mu\text{M}$, 11.5 ± 4.4 mV, $n = 10$, $p = 0.78$, vs. control; GSKa $10 \mu\text{M}$, 18.1 ± 2.5 mV, $n = 8$, $p = 0.21$, vs. control; Mann-Whitney U test) (Fig. 2D). Thus, GSKa slightly increases the activation and deactivation kinetics of TMEM16B that may account for some of the potentiating effects observed in the *Tout* current of the oocytes.

3.4. GSK2193874 on chloride currents mediated by TMEM16B channels

The potentiating effect of GSKa on CaCCs prompted us to test whether other TRPV4 modulating compounds have an effect on TMEM16B. Thus, we tested the TRPV4 channel antagonist GSK2193874 (GSKb) on HEK cells expressing TMEM16B. Sample recordings are shown in the presence of the minimal (1.5 nM) and maximal ($1.5 \mu\text{M}$)

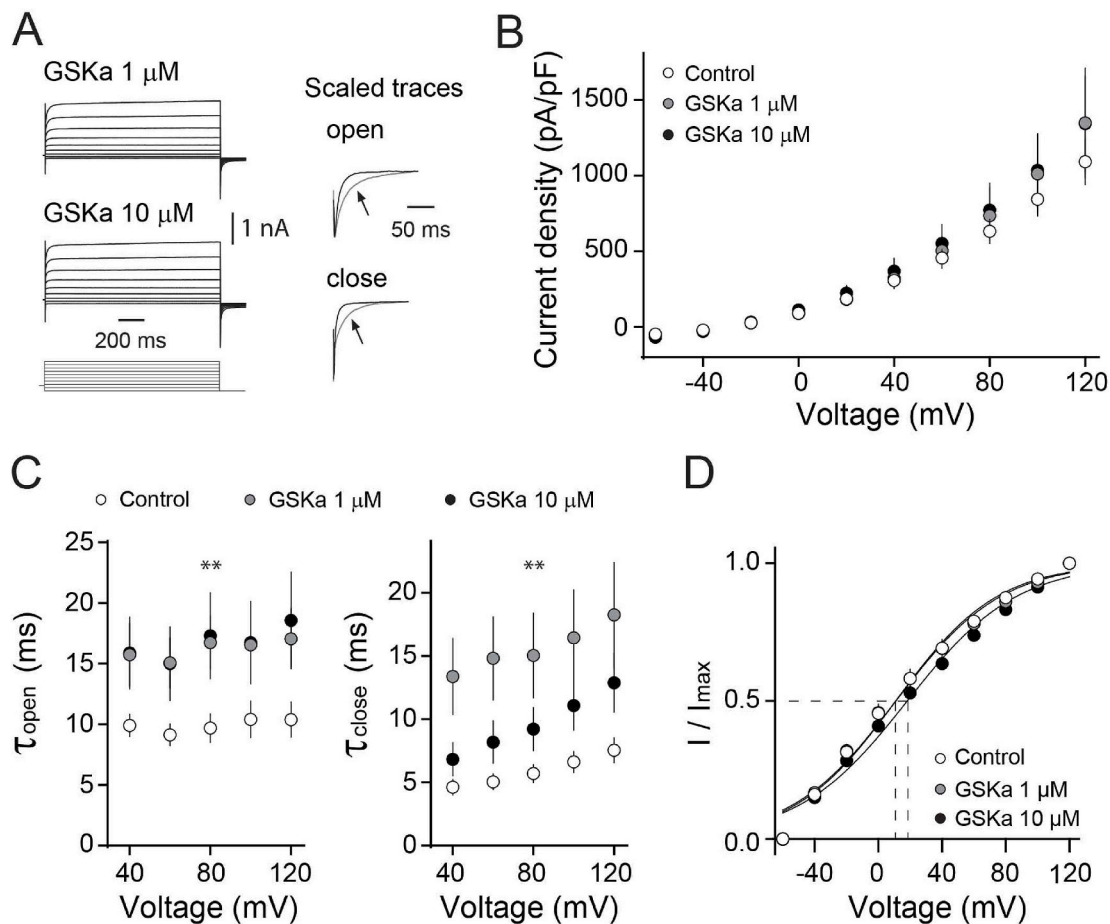


Fig. 3. GSK1016790A on TMEM16B currents in HEK293 cells. (A) Representative current traces induced by square voltage steps recorded in different GSK1016790A (GSKa) concentrations (1 and 10 μM). The right side of the panel shows the scaled traces superimposed and compared to the control (black) and GSKa 10 μM (gray, pointed by arrow). (B) Summary of the current-voltage relation at the steady state expressed as current density. The plot shows similar voltage activation in control and two different concentrations of GSKa. (C) Summary of the time constant of activation shows a significant increase at all voltages in presence of GSKa 1 μM ($*p < 0.05$, vs. control) and 10 μM ($**p < 0.001$, vs. control), similarly the deactivation time constant increased statistically significant at all voltages only for 1 μM GSKa ($**p < 0.001$, vs. control). (D) Summary of the normalized current voltage relation shows non-significant changes (dashed lines) on the curves fitted by the Boltzmann function (black lines). One-way ANOVA with multiple comparisons correction, Tukey's post-hoc. Symbols show mean \pm S.E.M.

concentrations of GSKb (Fig. 4A), which unexpectedly increased the currents generated by TMEM16B. A current-voltage relation was obtained from the steady state currents induced by square depolarizing voltages and expressed as current density for different GSKb concentrations, the maximal current amplitude obtained increased statistically significant at the maximal positive voltage used in a concentration dependent relation (control, 1011 ± 173.6 pA/pF, $n = 13$; GSKb 1.5 nM, 1133 ± 205.8 pA/pF, $n = 9$; GSKb 15 nM, 1408 ± 197.8 pA/pF, $n = 9$; GSKb 150 nM, 1958 ± 322.8 pA/pF, $*p = 0.0119$ vs. control, $n = 13$; GSKb 1.5 μM , 1935 ± 179.5 pA/pF, $**p = 0.002$ vs. control, $^{\&}p = 0.0133$ vs. GSKb 1.5 nM, $n = 10$; Mann-Whitney U test) (Fig. 4B). Activation time course shows statistically significant increases at 120 mV (control, 8.9 ± 0.63 ms, $n = 13$; GSKb 1.5 nM, 17.1 ± 2.25 ms, $***p = 0.0006$ Vs. control, $n = 9$; GSKb 15 nM, 10.5 ± 0.9 ms, $p = 0.137$, $n = 9$; GSKb 150 nM, 12.7 ± 1.5 ms, $*p = 0.029$ Vs. control, $n = 13$; GSKb 1.5 μM , 13.5 ± 1.6 ms, $**p = 0.0061$ Vs. control, $n = 8$; Unpaired student t -test Vs. control), without follow a concentration-dependent relation, similarly deactivation time course showed a significant increase at 120 mV mainly at higher concentrations (control, 3.0 ± 0.7 ms, $n = 13$; GSKb 1.5 nM, 7.5 ± 2.8 ms, $p = 0.085$, $n = 9$; GSKb 15 nM, 5.0 ± 1.2 ms, $p = 0.14$, $n = 9$; GSKb 150 nM, 8.5 ± 1.3 ms, $**p = 0.001$, $n = 13$; GSKb 1.5 μM , 8.0 ± 1.5 ms, $**p = 0.003$, $n = 8$; Unpaired student t -test Vs. control) (Fig. 4C). This result indicates a pharmacological potentiation of the TMEM16B chloride currents by GSKb at nanomolar concentrations.

A concentration-response relation was constructed normalizing TMEM16B mediated currents in presence of GSKb to the current measured in absence of any drug. EC_{50} was obtained by a dose-response fitting function. Fitted curves showed an increase of the EC_{50} at more positive voltages (40 mV, $EC_{50} = 9.4$ nM; 120 mV, $EC_{50} = 24.2$ nM) and the efficacy is decreased judged by the percent of stimulation response (40 mV, $224 \pm 21\%$; 120 mV, $198 \pm 20\%$) suggesting a voltage-dependent effect without changing the Hill number (40 mV, 0.95; 120 mV, 0.9), however it was not statistically significant (Fig. 4D). Boltzmann function did not show a significant change on the voltage dependency at all different GSKb concentrations (data not shown). This result indicates that GSKb acts as a positive modulator of the TMEM16B mediated currents without affecting the channel open probability or voltage dependency.

4. Discussion

Selective pharmacological compounds affecting CaCCs have been difficult to identify, for example, some of the potent and selective inhibitors proposed for CaCCs produce a pharmacological effect on some TRPs [37,38] and even the most potent TMEM16A activator (E_{act}) was recently reported as an activator of the TRPV1 and TRPV4 channels [43, 45]. Physical and functional coupling between CaCCs with TRPVs have been already demonstrated in heterologous expression and in tissues

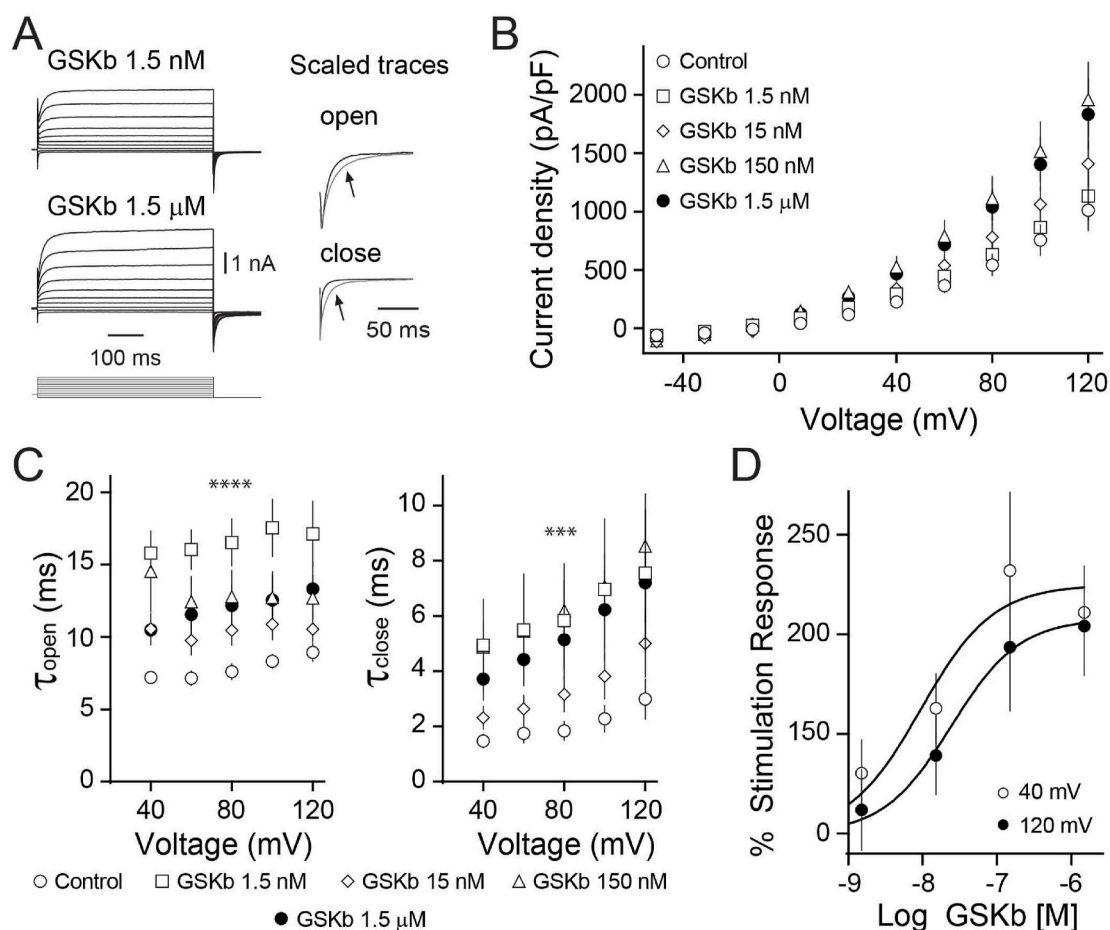


Fig. 4. GSK2193874 on TMEM16B currents in HEK293 cells. (A) Representative current traces induced by 20 mV square voltage steps in different GSK2193874 (GSKb) concentrations and scaled traces superimposed from control (black) and 1.5 μM GSKb (gray, pointed by arrow) are shown at the right side of the panel. (B) Summary of the current-voltage relation expressed as current density shows a clear increase on the current density in concentration dependent relation. (C) Summary of the time constant of activation shows a significant increase at all voltages explored in presence of GSKb compared to control without follow a concentration dependent relation (****p < 0.0001, GSKb 1.5 nM; *p < 0.05, GSKb 150 nM; *p < 0.05, GSKb 1.5 μM), except for 15 nM. Similarly, the deactivation time constant increases statistically significant at all voltages without follow a concentration dependent relation compared to control (**p < 0.01, GSKb 1.5 nM; ***p < 0.001, GSKb 150 nM; **p < 0.01, GSKb 1.5 μM) except for 15 nM. (D) Concentration-response curve shows the percent of stimulation response respect to control at 40 (empty circles) and 120 mV (filled circles). Curve fitted indicates an EC_{50} at the nanomolar concentrations (black lines). One-way ANOVA with multiple comparisons correction, Tukey's post-hoc. Symbols show mean \pm S.E.M.

[43,44,52]. Studies to elucidate the possible pharmacological interaction of both channel families are essential to generate accurate conclusions, especially in tissues where both channels are expressed like in DRG, choroid plexus epithelial cells and retinal epithelium [26,44,45, 53–55].

Previous reports demonstrated that compounds initially described as selective for CaCCs also have effects on TRPVs [38,43,45]. Our study suggests that the case may operate the other way around, that is, TRPV selective compounds may affect CaCCs. Initially, we found a potentiation of the *X. laevis* oocyte *Tout* chloride current by the TRPV4 selective agonist GSK1016790A (GSKa). Since TRPV4 is not functionally expressed in intact oocytes [56,57], it was unlikely that the effect on the *Tout* current was due to an interaction of GSKa with TRPV4 channel, instead we hypothesized that the effect should be on the CaCCs. Cloned mouse TMEM16B was expressed in HEK293 cells was used to study the effect of the GSKa/b on CaCCs and niflumic acid induced a clear retardation on the activation and deactivation kinetics moving the channel open probability to more positive voltages without affecting the steady-state current amplitude. Similarly, GSKa 1 μM did not affect the current amplitude of cloned TMEM16B but caused a significant reduction on the deactivation kinetics, this result hardly explains the total effect on CaCCs in the oocytes, however, considering that TMEM16A

represents the main current component and participation on the fast block to polyspermy [58], future experiments on cloned TMEM16A channels are required to support this finding. GSKa micromolar concentrations used here constrain further pharmacological studies regarding the nanomolar concentrations required for TRPV4 channels [47].

On the other hand, we present experimental evidence indicating that the TRPV4 blocker GSK2193874 (GSKb) caused important changes in the chloride currents mediated by the mouse TMEM16B channel expressed in HEK293 cells. GSKb enhanced TMEM16B currents in a voltage dependent manner at nanomolar concentrations and reaches its maximal effect at 150 nM of GSK2193874. Here we found an $EC_{50} = 9$ and 24 nM close to the nanomolar concentrations ($IC_{50} = 3$ nM) reported for TRPV4 channels [46]. Thus, this compound is an attractive alternative to be used in the characterization of TMEM16B channels, however, studies about the effect of these molecules on TMEM16A are still required to rule out their selectivity, considering that some molecules show similar selectivity or differential effects on both channels [20,42].

In conclusion, this study describes the effect of two potent modulators of the TRPV4 channels on the CaCCs, specifically on cloned TMEM16B and further experiments are required to understand the *Tout* current enhancement in oocytes. Our findings suggest careful

interpretations of pharmacological studies performed on tissues where TRPV4 and TMEM16B channels co-express [55] and helps to achieve precise conclusions in preclinical studies about TRPV4. Finally, our observations indicate that the GSKa/b structures may be used as templates to design new potent and selective drugs for TMEM16B.

Author contributions

AH, AAP, JACV, AMT contributed to conception and design of the study. AH and JACV performed whole-cell voltage clamp experiments. AAP performed the two voltage-clamp recordings in Oocytes. AH organized the data and performed the statistical analysis. AH and AMT funding acquisition and wrote original draft preparation. All authors contributed to manuscript revision, read, and approved the submitted version.

Declaration of competing interest

The authors declare that they have no known competing financial interests or personal relationships that could have appeared to influence the work reported in this paper.

Acknowledgments

We thank A.E. Espino-Saldaña and E. Garay for providing technical assistance. AAP received PhD fellowship 342519 from CONACYT. JACV was a postdoctoral fellow from CONACYT. This work was supported by grants from PAPIIT-DGAPA-UNAM (TA 200217 and IN205321) to AH and CONACYT A1S7659 and PAPIIT IN204520 to AMT. The authors thank Jessica González Norris for editing the manuscript.

References

- [1] R. Miledi, A calcium-dependent transient outward current in *Xenopus laevis* oocytes, *Proc. R. Soc. Lond. Ser. B Biol. Sci.* 215 (1982) 491–497, <https://doi.org/10.1098/rspb.1982.0056>.
- [2] M.E. Barish, A transient calcium-dependent chloride current in the immature *Xenopus* oocyte, *J. physiol.* 342 (1983) 309–325, <https://doi.org/10.1113/jphysiol.1983.sp014852>.
- [3] C. Hartzell, I. Putzier, J. Arreola, Calcium-activated chloride channels, *Annu. Rev. Physiol.* 67 (2005) 719–758, <https://doi.org/10.1146/annurev.physiol.67.032003.154341>.
- [4] F. Huang, H. Zhang, M. Wu, H. Yang, M. Kudo, C.J. Peters, P.G. Woodruff, O. D. Solberg, M.L. Donne, X. Huang, D. Sheppard, J.V. Fahy, P.J. Wolters, B. L. Hogan, W.E. Finkbeiner, M. Li, Y.N. Jan, L.Y. Jan, J.R. Rock, Calcium-activated chloride channel TMEM16A modulates mucin secretion and airway smooth muscle contraction, *Proc. Natl. Acad. Sci. U.S.A.* 109 (2012) 16354–16359, <https://doi.org/10.1073/pnas.1214596109>.
- [5] K. Kunzelmann, V.M. Milenkovic, M. Spitzner, R.B. Soria, R. Schreiber, Calcium-dependent chloride conductance in epithelia: is there a contribution by Bestrophin? *Pflug. Arch. Eur. J. Physiol.* 454 (2007) 879–889, <https://doi.org/10.1007/s00424-007-0245-z>.
- [6] D. Guo, L. Young, C. Patel, Z. Jiao, Y. Wu, T. Liu, P.R. Kowey, G.X. Yan, Calcium-activated chloride current contributes to action potential alternations in left ventricular hypertrophy rabbit, *Am. J. Physiol. Heart Circ. Physiol.* 295 (2008) H97–H104, <https://doi.org/10.1152/ajpheart.01032.2007>.
- [7] S. Andre, H. Boukhaddaoui, B. Campo, M. Al-Jumaily, V. Mayeux, D. Greuet, J. Valmier, F. Scamps, Axotomy-induced expression of calcium-activated chloride current in subpopulations of mouse dorsal root ganglion neurons, *J. Neurophysiol.* 90 (2003) 3764–3773, <https://doi.org/10.1152/jn.00449.2003>.
- [8] H.R. Matthews, J. Reisert, Calcium, the two-faced messenger of olfactory transduction and adaptation, *Curr. Opin. Neurobiol.* 13 (2003) 469–475, [https://doi.org/10.1016/s0959-4388\(03\)00097-7](https://doi.org/10.1016/s0959-4388(03)00097-7).
- [9] J.E. Angermann, A.R. Sanguinetti, J.L. Kenyon, N. Leblanc, I.A. Greenwood, Mechanism of the inhibition of Ca²⁺-activated Cl⁻ currents by phosphorylation in pulmonary arterial smooth muscle cells, *J. Gen. Physiol.* 128 (2006) 73–87, <https://doi.org/10.1085/jgp.200609507>.
- [10] M.R. Lalonde, M.E. Kelly, S. Barnes, Calcium-activated chloride channels in the retina, *Channels* 2 (2008) 252–260, <https://doi.org/10.4161/chan.2.4.6704>.
- [11] A. Caputo, E. Caci, L. Ferrera, N. Pedemonte, C. Barsanti, E. Sondo, U. Pfeffer, R. Ravazzolo, O. Zegarra-Moran, L.J. Galletta, TMEM16A, a membrane protein associated with calcium-dependent chloride channel activity, *Science* 322 (2008) 590–594, <https://doi.org/10.1126/science.1163518>.
- [12] B.C. Schroeder, T. Cheng, Y.N. Jan, L.Y. Jan, Expression cloning of TMEM16A as a calcium-activated chloride channel subunit, *Cell* 134 (2008) 1019–1029, <https://doi.org/10.1016/j.cell.2008.09.003>.
- [13] Y.D. Yang, H. Cho, J.Y. Koo, M.H. Tak, Y. Cho, W.S. Shim, S.P. Park, J. Lee, B. Lee, B.M. Kim, R. Raouf, Y.K. Shin, U. Oh, TMEM16A confers receptor-activated calcium-dependent chloride conductance, *Nature* 455 (2008) 1210–1215, <https://doi.org/10.1038/nature07313>.
- [14] S. Dang, S. Feng, J. Tien, C.J. Peters, D. Bulkley, M. Lolicato, J. Zhao, K. Zuberbuhler, W. Ye, L. Qi, T. Chen, C.S. Craik, Y.N. Jan, D.L. Minor Jr., Y. Cheng, L.Y. Jan, Cryo-EM structures of the TMEM16A calcium-activated chloride channel, *Nature* 552 (2017) 426–429, <https://doi.org/10.1038/nature25024>.
- [15] C. Paulino, V. Kalienkova, A.K.M. Lam, Y. Neldner, R. Dutzler, Activation mechanism of the calcium-activated chloride channel TMEM16A revealed by cryo-EM, *Nature* 552 (2017) 421–425, <https://doi.org/10.1038/nature24652>.
- [16] J.A. Contreras-Vite, S. Cruz-Rangel, J.J. De Jesus-Perez, I.A. Figueroa, A. A. Rodriguez-Menchaca, P. Perez-Cornejo, H.C. Hartzell, J. Arreola, Revealing the activation pathway for TMEM16A chloride channels from macroscopic currents and kinetic models, *Pflug. Arch. Eur. J. Physiol.* 468 (2016) 1241–1257, <https://doi.org/10.1007/s00424-016-1830-9>.
- [17] S. Cruz-Rangel, J.J. De Jesus-Perez, J.A. Contreras-Vite, P. Perez-Cornejo, H. C. Hartzell, J. Arreola, Gating modes of calcium-activated chloride channels TMEM16A and TMEM16B, *J. physiol.* 593 (2015) 5283–5298, <https://doi.org/10.1113/JP271256>.
- [18] Q. Xiao, K. Yu, P. Perez-Cornejo, Y. Cui, J. Arreola, H.C. Hartzell, Voltage- and calcium-dependent gating of TMEM16A/ANO1 chloride channels are physically coupled by the first intracellular loop, *Proc. Natl. Acad. Sci. U.S.A.* 108 (2011) 8891–8896, <https://doi.org/10.1073/pnas.1102147108>.
- [19] S. Cruz-Rangel, J.J. De Jesus-Perez, I.A. Arechiga-Figueroa, A.A. Rodriguez-Menchaca, P. Perez-Cornejo, H.C. Hartzell, J. Arreola, Extracellular protons enable activation of the calcium-dependent chloride channel TMEM16A, *J. physiol.* 595 (2017) 1515–1531, <https://doi.org/10.1113/JP273111>.
- [20] C.M. Ta, K.E. Acheson, N.J.G. Rorsman, R.C. Jongkind, P. Tammaro, Contrasting effects of phosphatidylinositol 4,5-bisphosphate on cloned TMEM16A and TMEM16B channels, *Br. J. Pharmacol.* 174 (2017) 2984–2999, <https://doi.org/10.1111/bph.13913>.
- [21] J.J. De Jesus-Perez, S. Cruz-Rangel, A.E. Espino-Saldana, A. Martinez-Torres, Z. Qu, H.C. Hartzell, N.E. Corral-Fernandez, P. Perez-Cornejo, J. Arreola, Phosphatidylinositol 4,5-bisphosphate, cholesterol, and fatty acids modulate the calcium-activated chloride channel TMEM16A (ANO1), *Biochimica et biophysica acta, Mol. Cell Biol. Lipids* 1863 (2018) 299–312, <https://doi.org/10.1016/j.bbalip.2017.12.009>.
- [22] U. Duvvuri, D.J. Shiwarski, D. Xiao, C. Bertrand, X. Huang, R.S. Edinger, J.R. Rock, B.D. Harfe, B.J. Henson, K. Kunzelmann, R. Schreiber, R.S. Seethala, A.M. Eglhoff, X. Chen, V.W. Lui, J.R. Grandis, S.M. Gollin, TMEM16A induces MAPK and contributes directly to tumorigenesis and cancer progression, *Cancer Res.* 72 (2012) 3270–3281, <https://doi.org/10.1158/0008-5472.CAN-12-0475-T>.
- [23] X. Zeng, P. Huang, M. Chen, S. Liu, N. Wu, F. Wang, J. Zhang, TMEM16A regulates portal vein smooth muscle cell proliferation in portal hypertension, *Experimental Therapeut Med* 15 (2018) 1062–1068, <https://doi.org/10.3892/etm.2017.5466>.
- [24] M.M. Ma, M. Gao, K.M. Guo, M. Wang, X.Y. Li, X.L. Zeng, L. Sun, X.F. Lv, Y.H. Du, G.L. Wang, J.G. Zhou, Y.Y. Guan, TMEM16A contributes to endothelial dysfunction by facilitating Nox2 NADPH oxidase-derived reactive oxygen species generation in hypertension, *Hypertension* 69 (2017) 892–901, <https://doi.org/10.1161/HYPERTENSIONAHA.116.08874>.
- [25] U. Oh, J. Jung, Cellular functions of TMEM16/anocetamin, *Pflug. Arch. Eur. J. Physiol.* 468 (2016) 443–453, <https://doi.org/10.1007/s00424-016-1790-0>.
- [26] Y. Takayama, K. Shibasaki, Y. Suzuki, A. Yamanaka, M. Tominaga, Modulation of water efflux through functional interaction between TRPV4 and TMEM16A/anocetamin 1, *Faseb. J. : Official Pub. Federation Am Societies Experimental Biol.* 28 (2014) 2238–2248, <https://doi.org/10.1096/fj.13-243436>.
- [27] B. Wang, C. Li, R. Huai, Z. Qu, Overexpression of ANO1/TMEM16A, an arterial Ca²⁺-activated Cl⁻ channel, contributes to spontaneous hypertension, *J. Mol. Cell. Cardiol.* 82 (2015) 22–32, <https://doi.org/10.1016/j.yjmcc.2015.02.020>.
- [28] A. Britschgi, A. Bill, H. Brinkhaus, C. Rothwell, I. Clay, S. Duss, M. Rebhan, P. Raman, C.T. Guy, K. Wetzel, E. George, M.O. Popa, S. Lilley, H. Choudhury, M. Gosling, L. Wang, S. Fitzgerald, J. Borawski, J. Baffoe, M. Labow, L.A. Gaither, M. Bentires-Alj, Calcium-activated chloride channel ANO1 promotes breast cancer progression by activating EGFR and CAMK signaling, *Proc. Natl. Acad. Sci. U.S.A.* 110 (2013) E1026–1034, <https://doi.org/10.1073/pnas.1217072110>.
- [29] D. Crottes, L.Y. Jan, The multifaceted role of TMEM16A in cancer, *Cell Calcium* 82 (2019) 102050, <https://doi.org/10.1016/j.ceca.2019.06.004>.
- [30] Z. Qu, W. Yao, R. Yao, X. Liu, K. Yu, C. Hartzell, The Ca(2+)-activated Cl(-) channel, ANO1 (TMEM16A), is a double-edged sword in cell proliferation and tumorigenesis, *Cancer Med.* 3 (2014) 453–461, <https://doi.org/10.1002/cam4.232>.
- [31] W. Namkung, P.W. Phuan, A.S. Verkman, TMEM16A inhibitors reveal TMEM16A as a minor component of calcium-activated chloride channel conductance in airway and intestinal epithelial cells, *J. Biol. Chem.* 286 (2011) 2365–2374, <https://doi.org/10.1074/jbc.M110.175109>.
- [32] S.J. Oh, S.J. Hwang, J. Jung, K. Yu, J. Kim, J.Y. Choi, H.C. Hartzell, E.J. Roh, C. J. Lee, MONNA, a potent and selective blocker for transmembrane protein with unknown function 16/anocetamin-1, *Mol. Pharmacol.* 84 (2013) 726–735, <https://doi.org/10.1124/mol.113.087502>.
- [33] A.J. Davis, J. Shi, H.A. Pritchard, P.S. Chadha, N. Leblanc, G. Vasilikostas, Z. Yao, A.S. Verkman, A.P. Albert, I.A. Greenwood, Potent vasorelaxant activity of the TMEM16A inhibitor T16A(inh)-A01, *Br. J. Pharmacol.* 168 (2013) 773–784, <https://doi.org/10.1111/j.1476-5381.2012.02199.x>.

- [34] R. De La Fuente, W. Namkung, A. Mills, A.S. Verkman, Small-molecule screen identifies inhibitors of a human intestinal calcium-activated chloride channel, *Mol. Pharmacol.* 73 (2008) 758–768, <https://doi.org/10.1124/mol.107.043208>.
- [35] R.C. Hogg, Q. Wang, W.A. Large, Effects of Cl channel blockers on Ca-activated chloride and potassium currents in smooth muscle cells from rabbit portal vein, *Br. J. Pharmacol.* 111 (1994) 1333–1341, <https://doi.org/10.1111/j.1476-5381.1994.tb14891.x>.
- [36] A. Gradogna, M. Pusch, Molecular pharmacology of kidney and inner ear CLC-K chloride channels, *Front. Pharmacol.* 1 (2010) 130, <https://doi.org/10.3389/fphar.2010.00130>.
- [37] H. Hu, J. Tian, Y. Zhu, C. Wang, R. Xiao, J.M. Herz, J.D. Wood, M.X. Zhu, Activation of TRPA1 channels by fenamate nonsteroidal anti-inflammatory drugs, *Pflug. Arch. Eur. J. Physiol.* 459 (2010) 579–592, <https://doi.org/10.1007/s00424-009-0749-9>.
- [38] R. Guinamard, C. Simard, C. Del Negro, Flufenamic acid as an ion channel modulator, *Pharmacol. Ther.* 138 (2013) 272–284, <https://doi.org/10.1016/j.pharmthera.2013.01.012>.
- [39] M. Reinsprecht, M.H. Rohn, R.J. Spadinger, I. Pecht, H. Schindler, C. Romanin, Blockade of capacitive Ca²⁺ influx by Cl⁻ channel blockers inhibits secretion from rat mucosal-type mast cells, *Mol. Pharmacol.* 47 (1995) 1014–1020.
- [40] H.S. Wang, J.E. Dixon, D. McKinnon, Unexpected and differential effects of Cl⁻ channel blockers on the Kv4.3 and Kv4.2 K⁺ channels. Implications for the study of the I(to2) current, *Circ. Res.* 81 (1997) 711–718, <https://doi.org/10.1161/01.res.81.5.711>.
- [41] J.M. Doughty, A.L. Miller, P.D. Langton, Non-specificity of chloride channel blockers in rat cerebral arteries: block of the L-type calcium channel, *J. physiol.* 507 (Pt 2) (1998) 433–439, <https://doi.org/10.1111/j.1469-7793.1998.433bt.x>.
- [42] Y. Seo, H.K. Lee, J. Park, D.K. Jeon, S. Jo, M. Jo, W. Namkung, Ani9, A novel potent small-molecule ANO1 inhibitor with negligible effect on ANO2, *PLoS One* 11 (2016), e0155771, <https://doi.org/10.1371/journal.pone.0155771>.
- [43] S. Liu, J. Feng, J. Luo, P. Yang, T.J. Brett, H. Hu, Eact, a small molecule activator of TMEM16A, activates TRPV1 and elicits pain- and itch-related behaviours, *Br. J. Pharmacol.* 173 (2016) 1208–1218, <https://doi.org/10.1111/bph.13420>.
- [44] Y. Takayama, D. Uta, H. Furue, M. Tominaga, Pain-enhancing mechanism through interaction between TRPV1 and anoctamin 1 in sensory neurons, *Proc. Natl. Acad. Sci. U.S.A.* 112 (2015) 5213–5218, <https://doi.org/10.1073/pnas.1421507112>.
- [45] M. Genovese, A. Borrelli, A. Venturini, D. Guidone, E. Caci, G. Viscido, G. Gambardella, D. di Bernardo, P. Scudieri, L.J.V. Galletta, TRPV4 and purinergic receptor signalling pathways are separately linked in airway epithelia to CFTR and TMEM16A chloride channels, *J. physiol.* 597 (2019) 5859–5878, <https://doi.org/10.1113/JP278784>.
- [46] K.S. Thorneloe, M. Cheung, W. Bao, H. Alsaïd, S. Lenhard, M.Y. Jian, M. Costell, K. Maniscalco-Hauk, J.A. Krawiec, A. Olzinski, E. Gordon, I. Lozinskaya, L. Elefante, P. Qin, D.S. Matasic, C. James, J. Tunstead, B. Donovan, L. Kallal, A. Waszkiewicz, K. Vaidya, E.A. Davenport, J. Larkin, M. Burgert, L.N. Casillas, R. W. Marquis, G. Ye, H.S. Eidam, K.B. Goodman, J.R. Toomey, T.J. Roethke, B. M. Jucker, C.G. Schnackenberg, M.I. Townsley, J.J. Lepore, R.N. Willette, An orally active TRPV4 channel blocker prevents and resolves pulmonary edema induced by heart failure, *Sci. Transl. Med.* 4 (2012) 159ra148, <https://doi.org/10.1126/scitranslmed.3004276>.
- [47] K.S. Thorneloe, A.C. Sulpizio, Z. Lin, D.J. Figueroa, A.K. Clouse, G.P. McCafferty, T. P. Chendrimada, E.S. Lashinger, E. Gordon, L. Evans, B.A. Misajet, D.J. Demarini, J. H. Nation, L.N. Casillas, R.W. Marquis, B.J. Votta, S.A. Sheardown, X. Xu, D. P. Brooks, N.J. Laping, T.D. Westfall, N-((1S)-1-[[4-((2S)-2-[[2,4-dichlorophenyl]sulfonyl]amino)-3-hydroxypropanoyl]-1-piperazinyl]carbonyl)-3-methylbutyl)-1-benzothiothiophene-2-carboxamide (GSK1016790A), a novel and potent transient receptor potential vanilloid 4 channel agonist induces urinary bladder contraction and hyperactivity: Part I, *J. Pharmacol. Exp. Therapeut.* 326 (2008) 432–442, <https://doi.org/10.1124/jpet.108.139295>.
- [48] S. Pifferi, M. Dibattista, A. Menini, TMEM16B induces chloride currents activated by calcium in mammalian cells, *Pflug. Arch. Eur. J. Physiol.* 458 (2009) 1023–1038, <https://doi.org/10.1007/s00424-009-0684-9>.
- [49] T.L. Toft-Bertelsen, D. Krizaj, N. MacAulay, When size matters: transient receptor potential vanilloid 4 channel as a volume-sensor rather than an osmo-sensor, *J. physiol.* 595 (2017) 3287–3302, <https://doi.org/10.1113/JP274135>.
- [50] R.H. Ryu, S.J. Oh, R.M. Lee, S.W. Jeong, L.Y. Jan, C.H. Lee, C.J. Lee, S.M. Jeong, Cloning and heterologous expression of new xANO2 from *Xenopus laevis*, *Biochem. Biophys. Res. Commun.* 408 (2011) 559–565, <https://doi.org/10.1016/j.bbrc.2011.04.060>.
- [51] Z. Qu, H.C. Hartzell, Functional geometry of the permeation pathway of Ca²⁺-activated Cl⁻ channels inferred from analysis of voltage-dependent block, *J. Biol. Chem.* 276 (2001) 18423–18429, <https://doi.org/10.1074/jbc.M101264200>.
- [52] H. Cho, Y.D. Yang, J. Lee, B. Lee, T. Kim, Y. Jang, S.K. Back, H.S. Na, B.D. Harfe, F. Wang, R. Raouf, J.N. Wood, U. Oh, The calcium-activated chloride channel anoctamin 1 acts as a heat sensor in nociceptive neurons, *Nat. Neurosci.* 15 (2012) 1015–1021, <https://doi.org/10.1038/nn.3111>.
- [53] S. Keckeis, N. Reichhart, C. Roubeix, O. Strauss, Anoctamin2 (TMEM16B) forms the Ca(2+)-activated Cl(-) channel in the retinal pigment epithelium, *Exp. Eye Res.* 154 (2017) 139–150, <https://doi.org/10.1016/j.exer.2016.12.003>.
- [54] P.Y. Zhao, G. Gan, S. Peng, S.B. Wang, B. Chen, R.A. Adelman, L.J. Rizzolo, TRP channels localize to subdomains of the apical plasma membrane in human fetal retinal pigment epithelium, *Investigative Ophthalmology vis. sci.* 56 (2015) 1916–1923, <https://doi.org/10.1167/iovs.14-15738>.
- [55] J.J. Tong, P. Acharya, L. Ebihara, Calcium-activated chloride channels in newly differentiating mouse lens fiber cells and their role in volume regulation, *Investigative Ophthalmology vis. sci.* 60 (2019) 1621–1629, <https://doi.org/10.1167/iovs.19-26626>.
- [56] A.D. Guler, H. Lee, T. Iida, I. Shimizu, M. Tominaga, M. Caterina, Heat-evoked activation of the ion channel, TRPV4, *J. Neurosci. : Official J Society Neurosci.* 22 (2002) 6408–6414, 20026679.
- [57] S. Loukin, Z. Su, X. Zhou, C. Kung, Forward genetic analysis reveals multiple gating mechanisms of TRPV4, *J. Biol. Chem.* 285 (2010) 19884–19890, <https://doi.org/10.1074/jbc.M110.113936>.
- [58] K.L. Wozniak, W.A. Phelps, M. Tembo, M.T. Lee, A.E. Carlson, The TMEM16A channel mediates the fast polyspermy block in *Xenopus laevis*, *J. Gen. Physiol.* 150 (2018) 1249–1259, <https://doi.org/10.1085/jgp.201812071>.